Bone Reports 8 (2018) 147–155

Contents lists available at ScienceDirect

Bone Reports

journal homepage: www.elsevier.com/locate/bonr

Deletion of Orai1 leads to bone loss aggravated with aging and impairs function of osteoblast lineage cells

Hyewon Choi[a,1,2], Sonal Srikanth[b], Elisa Atti[a], Flavia Q. Pirih[c], Jeanne M. Nervina[d,3], Yousang Gwack[b], Sotirios Tetradis[e,*]

[a] Division of Oral Biology and Medicine, School of Dentistry, University of California at Los Angeles, 10833 Le Conte Ave., Los Angeles, CA 90095-1668, United States
[b] Department of Physiology, David Geffen School of Medicine, University of California at Los Angeles, 10833 Le Conte Avenue, Los Angeles, CA 90095-1751, United States
[c] Section of Periodontics, School of Dentistry, University of California at Los Angeles, 10833 Le Conte Ave., Los Angeles, CA 90095-1668, United States
[d] Section of Orthodontics, School of Dentistry, University of California at Los Angeles, 10833 Le Conte Ave., Los Angeles, CA 90095-1668, United States
[e] Division of Diagnostic and Surgical Sciences, School of Dentistry, University of California at Los Angeles, 10833 Le Conte Ave., Los Angeles, CA 90095-1668, United States

ARTICLE INFO

Keywords:
Orai1
Osteoblast lineage cells
Bone
Knockout mice

ABSTRACT

Osteoblast lineage cells, a group of cells including mesenchymal progenitors, osteoblasts, and osteocytes, are tightly controlled for differentiation, proliferation and stage-specific functions in processes of skeletal development, growth and maintenance. Recently, the plasma membrane calcium channel Orai1 was highlighted for its role in skeletal development and osteoblast differentiation. Yet the roles of Orai1 in osteoblast lineage cells at various stages of maturation have not been investigated. Herein we report the severe bone loss that occurred in Orai1 −/− mice, aggravated by aging, as shown by the microcomputed tomography (mCT) and bone histomorphometry analysis of 8-week and 12-week old Orai1 −/− mice and sex-matched WT littermates. We also report that Orai1 deficiency affected the differentiation, proliferation, and type I collagen secretion of primary calvarial osteoblasts, mesenchymal progenitors, and osteocytes in Orai1 −/− mice; specifically, our study revealed a significant decrease in the expression of osteocytic genes Fgf23, DMP1 and Phex in the cortical long bone of Orai1 −/− mice; a defective cellular and nuclear morphology of Orai1 −/− osteocytes; and defective osteogenic differentiation of Orai1 −/− primary calvarial osteoblasts (pOBs), including a decrease in extracellular-secretion of type I collagen. An increase in the mesenchymal progenitor population of Orai1 −/− bone marrow cells was indicated by a colony forming unit-fibroblasts (CFU-F) assay, and the increased proliferation of Orai1 −/− pOBs was indicated by an MTT assay. Notably, Orai1 deficiency reduced the nuclear localization and transcription activity of the Nuclear Factor of Activated T-cell c1 (NFATc1), a calcium-regulated transcription factor, in pOBs. Altogether, our study demonstrated the crucial role of Orai1 in bone development and maintenance, *via* its diverse effects on osteoblast lineage cells from mesenchymal progenitors to osteocytes.

1. Introduction

Throughout the life of an organism, bone is remodeled and maintained by tightly controlled bone resorption and bone formation. Bone formation has been known to be mediated primarily by osteoblasts, the main bone-forming cells of the osteoblast lineage (Kronenberg, 2016). Recent studies reveal the crucial roles of other osteoblast lineage cells such as mesenchymal progenitors and osteocytes in mineral and bone homeostasis (Dallas et al., 2013; Ono and Kronenberg, 2015). Thus a stringent regulation of the osteoblast lineage, from progenitors to osteocytes, is essential to ensure proper bone formation and homeostasis at local and systemic levels.

For the molecular machinery involved in osteoblast biology, a plasma membrane calcium channel, Orai1, was recently identified for its role in bone homeostasis (Robinson et al., 2012; Hwang and Putney, 2012; Hwang et al., 2012). Upon calcium storage depletion in the endoplasmic reticulum (ER), Orai1 is activated and allows a rapid and transient calcium influx, called store-operated calcium entry (SOCE), to

* Corresponding author.
E-mail addresses: choi.1502@osu.edu (H. Choi), ssrikanth@mednet.ucla.edu (S. Srikanth), eatti@dentistry.ucla.edu (E. Atti), fpirih@dentistry.ucla.edu (F.Q. Pirih), j.nervina@nyu.edu (J.M. Nervina), ygwack@mednet.ucla.edu (Y. Gwack), stetradis@dentistry.ucla.edu (S. Tetradis).
[1] First author.
[2] Present address: Department of Veterinay Bioscience, College of Veterinary Medicine, The Ohio State University, 1900 Coffey Road, Columbus, OH 43210.
[3] Present address: College of Dentistry, New York University, 421 First Avenue, New York, NY 10010.

https://doi.org/10.1016/j.bonr.2018.03.007
Received 22 November 2017; Received in revised form 21 March 2018; Accepted 22 March 2018
Available online 05 April 2018

the cytoplasm (Feske et al., 2006). Genetic disruption of Orai1 impaired the skeletal development of 3 week-old mice and resulted to the osteopenia with decreased bone mineral density in adult mice due to significantly defective osteoblastic bone formation overriding defective osteoclastic bone resorption (Robinson et al., 2012; Hwang et al., 2012). As a cellular mechanism underlying a decreased bone density of Orai1 −/− mice, defective osteoblast differentiation was suggested based on the *in vitro* differentiation assay using Orai1 −/− bone marrow stromal cells and the osteoblast cell line (Robinson et al., 2012; Hwang et al., 2012). Yet the impact of Orai1 deficiency on various osteoblast lineage cells and their cumulative contributions to bone homeostasis have not been fully investigated, limiting our understanding of Orai1 in bone biology.

Herein, we show that Orai1 is broadly involved in differentiation, proliferation, and function of various osteoblast lineage cells. Orai1 deficiency impacted differentiation of osteoblast lineage cells from progenitors to osteocytes, indicated by the increased progenitor population within Orai1 −/− bone marrow cells and the morphologically defective osteocytes in Orai1 −/− mice. Orai1 deficiency also affected the secretory function of primary calvarial osteoblasts (pOBs), leading to a decrease in the amount of extracellular mature type I collagen. Moreover, Orai1 deficiency in pOBs led to an increase in *in-vitro* proliferation, which corroborates an increase in the number of osteoblasts per bone perimeter in Orai1 −/− mice. Also, defective activation of Nuclear Factor of Activated T-cell c1 (NFATc1), a calcium-regulated transcription factor, was observed in Orai1 −/− pOBs, suggesting that defective SOCE resulting from Orai1 deficiency may impact various calcium signaling pathways in osteoblasts. These diverse effects of Orai1 deficiency imply that Orai1 is a critical regulator of cellular functions of osteoblast lineage cells, emphasizing the importance of intracellular Ca^{2+}-homeostasis in osteoblast biology, bone homeostasis, and other degenerative bone disorders.

2. Materials and methods

2.1. Mice

Orai1 −/− mice were generated by Dr. Yousang Gwack (University of California, Los Angeles) as previously described (Kim et al., 2011). Mice were genotyped by PCR of tail DNA as previously described (Gwack et al., 2008). All mice were maintained in pathogen-free barrier facilities and used in accordance with the protocols approved by the Institutional Animal Care and Use Committee at the University of California, Los Angeles.

2.2. Microcomputed tomography (μCT) and bone histomorphometry analysis

μCT were performed on femur and vertebrae as previously described (16 μm resolution) (Aghaloo et al., n.d.-a), using a Scanco μCT40 scanner (Scanco Medical, Switzerland). Visualization, reconstruction, and volume analysis of the data were performed using the Metamorph Imaging system (Universal Imaging, USA). Histomorphometric analysis of femurs was performed at the histomorphometry core laboratory (UCLA), following previously described protocols (Hsu et al., 2008). For both analyses, samples were isolated from *Orai1 −/−* mice and sex-matched WT littermates.

2.3. Scanning Electron Microscopy (SEM) analysis

The analysis was performed at UCLA department of materials science and engineering core facility using a Nova NanoSEM 230 scanning electron microscope (FEI, USA) with field emission gun and variable pressure capabilities equipped with backscattered electron detectors and an energy dispersive x-ray spectrometer (ThermoScientific, USA). Femur samples from 8-week old *Orai1 −/−* male mice and sex-matched WT littermate were fixed in 4% Glutaraldehyde overnight at 4′C, non-decalcified, resin-casted and coronal-sectioned at the distal metaphyseal area, sputter-coated with gold palladium, and subsequently examined with SEM.

2.4. Primary cell isolation and culture

pOBs were isolated from fetal or neonatal *Orai1 −/−* mice and WT littermates following the previously described protocol (Tetradis et al., 2001). Mice were individually marked, kept alive until the completion of PCR genotyping of tail DNA. Calvaria from Orai1 −/− and WT mice were separated for cell isolation. Bone marrow stromal cells (BMSCs) were isolated from long bones of 8–12 week old *Orai1 −/−* mice and WT littermates as previously described (Aghaloo et al., n.d.-b). Mesenchymal progenitors were isolated from BMSCs following the published protocol using frequent medium changes for progenitor separation (Soleimani and Nadri, 2009). For proliferation, cells were plated at the concentration of 40,000 cells/ml and cultured in DMEM (ThermoFisher scientific, Waltham, MA) with 10% FBS, 100 units/ml penicillin and 100 μg/ml streptomycin. For osteoblastic differentiation, confluent pOBs and BMSCs cultured in proliferation medium were changed to osteogenic medium, which was α-MEM (Invitrogen, Carlsbad, CA) with 10% FBS, 100 units/ml penicilin,100 μg/ml streptomycin supplemented with 50 μg/ml ascorbic acid (Sigma, St. Louis, MO, USA) and 10 mM beta-glycerophosphate (Sigma, St. Louis, MO, USA). Media were replaced every 2–3 days.

2.5. In vitro osteogenic differentiation assays

pOBs and BMSCs cultured in osteogenic medium for designated days were fixed with 4% paraformaldehyde and stained for Alkaline phosphatase, Alizarin Red, and Von Kossa stainings as previously described (Aghaloo et al., n.d.-b).

2.6. RNA extraction and real-time quantitative PCR (qPCR)

RNA was extracted from cultured cells or compact long bones isolated from using triazol (Invitrogen, Carlsbad, CA) and prepared for qPCR as previously described (Pirih et al., 2008). The sequences of gene-specific primers for qPCR are listed in Supplementary Table 1.

2.7. Western blot analysis

Western blot with anti-type I collagen antibody (Santa Cruz Biotechnology) was performed using pepsin-digested extracts and total cell lysates prepared from pOBs cultured in osteogenic medium for 3 weeks, following the published protocol for intracellular and extracellular type I collagen (Zhao et al., 2008).

2.8. Colony-forming unit (CFU) assay

Cells were isolated from bone marrow cells following the published protocol (Soleimani and Nadri, 2009), plated at the very low density of 10,000 cells/well in 6 well plate, cultured in proliferation medium for 10 days and prepared for Giemsa staining to increase the visibility for counting CFUs. Colonies containing > 50 cells were determined under the microscope, considered as CFUs.

2.9. 3-(4,5-Dimethylthiazol-2-yl)-2,5-diphenyltetrazolium bromide (MTT) assay and cell counting assay

For MTT assay, pOBs were plated at 20,000 cells per well of 96-well plate in triplicates, cultured for 12 h, and subjected to the assay using an MTT kit (Cayman Chemical Company, Ann Arbor, MI) following the manufacturer's protocol. For cell counting assay, pObs were plated at 20,000 cells per well of 24-well plate in duplicates, cultured for designated days, harvested by brief trypsin treatment, centrifuged and re-suspended to stain with toluidine blue for viable cell counting.

2.10. Monitoring of intracellular free Ca^{2+} concentrations

Optical monitoring of intracellular Ca^{2+} concentration was performed as previously described (Gwack et al., 2008). pOBs were seeded onto #1 glass coverslips in 24 well plate and cultured overnight. For Ca^{2+} monitoring, the medium was changed into Ca^{2+} free HBSS solution and loaded with 5 μM Fura-2, a quantifiable fluorescent Ca^{2+} dye. Imaging was performed with the Metamorph/Metafluor system (Universal Imaging). Each trace is an average of at least 30–40 osteoblasts. To induce SOCE, intracellular Ca^{2+} storage was depleted by 1 μM thapsigargin (Sigma, St. Louis, MO) treatment and the Ca^{2+} solution was introduced into the HBSS solution for extracellular Ca^{2+} supply. To inhibit SOCE, 100 μM of 2-aminoethoxydiphenyl borate (2-APB), a SOC channel blocker, (Sigma, St. Louis, MO) was added to the HBSS solution.

2.11. NFAT immunocytochemistry

pOBs were plated at 40,000 cells/ml per chamber of poly-L-lysine-coated glass 4-chamber slides and cultured for 24 h. Subconfluent cells were fixed with 4% paraformaldehyde for 10 min, permeabilized with 0.1% Triton X-100/PBS for 5 min, saturated with 0.5% bovine serum albumin, and incubated with 1.0 μg/ml anti-NFATc1 mAb 7A6 (Santa Cruz Biotechnology) for 1 h at room temperature, then after washing with PBS stained with Alexa Fluor 488-conjugated goat anti-mouse IgG (BDbioscience, San Jose) for 1 h at RT. After washing, cells were counterstained with the DNA-intercalating dye DAPI (4,6-diamidino-2-phenylindole), mounted with coverslips using Vectashield (Vector Laboratories), and observed under a Nikon Inverted Stage fluorescent microscope (Nikon).

2.12. Luciferase reporter assay

Transient transfection of luciferase plasmid to pOBs was performed using Lipofectin with Plus reagents (ThermoFisher Scientific, Waltham, MA) following the manufacturer's protocol. pTL luciferase plasmid containing three tandem repeats of NFAT/AP-1 consensus binding sites in its promoter was provided by Dr. Yousang Gwack. Then at 48 h after transfection, cells were stimulated with 25 nM PMA and 1 μM Ionomycin for 6 h, collected in luciferase lysis buffer and subsequently processed for the luciferase assay (Promega, Madicine, WI) following the manufacturer's protocol.

2.13. Statistical analysis

All values are presented as mean ± standard error of the mean (SEM) from at least 3 independent experiments. Data were analyzed with the paired two-tailed Student's *t*-tests as appropriate for the data set. A *p*-value < 0.05 was considered as statistically significant.

3. Results

3.1. Age-related bone loss in Orai1 −/− mice

To evaluate the effect of Orai1 deficiency on the overall bone formation, we performed quantitative microcomputed tomography (μCT) analysis for femurs and lumbar vertebrae (L4) of 8 week-old *Orai1* −/− mice and sex-matched WT littermate controls. A severe osteoporotic bone phenotype of Orai1 −/− mice was indicated, as *Orai1* −/− mice presented a lower trabecular bone mass in both femur and lumbar vertebrae (Fig. 1A and B), and a significant decrease in bone volume *versus* tissue volume (BV/TV), trabecular bone thickness (Tb.Th), and trabecular number (Tb.N.) (Fig. 1C). In addition to these quantitative defects, qualitative bone defects were also observed in Orai1 −/− mice, shown as a significant decrease in bone mineral density (BMD) of both metaphyseal trabecular bone (Fig. 1C). The previous study of 3-week old *Orai1* −/− mice only showed a very mild effect of Orai1 deficiency on bone (Robinson et al., 2012). While perinatal *Orai1* −/− mice did not present obvious defects in cartilage and bone formation when examined with histological analysis and skeletal preparation (Sup Fig. 1), 8-week old *Orai1* −/− mice presented significant bone loss, indicated by μCT analysis. This led us to examine whether the effect of Orai1 deficiency on bone is age-related or not. Therefore, 8-week and 12-week old *Orai1* −/− mice with their WT littermate controls were analyzed with bone histomorphometry (Fig. 1D). Results indicated that bone loss in *Orai1* −/− mice was aggravated by aging, as deterioration of trabecular bone volume (BV/TV) in distal femoral metaphyseal area was significantly greater at 12-week postnatal than the one at-8 week. Consistent with the μCT findings, the static parameters of histomorphometry also indicated a severe osteoporotic bone phenotype of *Orai1* −/− mice, shown by a significant decrease in bone volume *versus* tissue volume (BV/TV), trabecular bone thickness (Tb.Th), and a significant increase in trabecular spacing (Tb.Sp.) (Fig. 1D).

3.2. Defective morphology of osteocytes in Orai1 −/− mice

Previous studies indicated that decreased bone mass of *Orai1* −/− mice resulted from decreased osteoblastic bone formation, rather than increased osteoclastic bone resorption (Ono and Kronenberg, 2015; Hwang et al., 2012), yet it remained largely unidentified whether Orai1 affects osteoblastic lineage cells from mesenchymal progenitors to mature osteocytes. In bone, osteocytes consist > 90% of bone cells and play a major regulatory role in bone matrix mineralization and bone remodeling by cell-to-cell interactions and secretion of organic and inorganic factors (Dallas et al., 2013). To identify whether Orai1 deficiency affects osteocytes or not, we first examined the cellular and nuclei morphology of osteocytes in *Orai1* −/− mice.

Scanning Electron Microscope (SEM) analysis revealed that osteocytes in *Orai1* −/− mice were narrowed and ragged in shape, compared to WT cells that were oval or round (Fig. 2A&B). Osteocytes in *Orai1* −/− mice were also detached from its lacunae, exhibiting abnormal pericellular space between the cell and mineralized bone surface. This feature may be related to defective mineralization of *Orai1* −/− mice, as the peri-osteocytic space has been shown to contain mineralizing extracellular matrix (Wysolmerski, 2013; Alcobendas et al., 1991). For the nuclei morphology, osteocytes in *Orai1* −/− mice presented smaller nuclei compared to WT (Fig. 2C). Osteocytes in *Orai1* −/− mice also presented significantly less euchromatin, shown as the electron-lucent area in the nuclei. As euchromatin is the area of loose chromatin allowing active gene transcription, this suggested that osteocytes in *Orai1* −/− mice could be less active in gene transcription and protein synthesis compared to WT (Palumbo, 1986). Then, we further examined whether Orai1 deficiency affects gene expression in osteocytes. For qPCR analysis, RNAs were extracted from the cortical long bone of 12 week-old *Orai1* −/− and WT littermate control and prepared for the analysis. As expected, Orai1 expression was ablated in the samples from *Orai1* −/− mice (Fig. 2D). Osteocytic gene expression was also decreased in *Orai1* −/− mice, as *Fgf23* and *Phex* were statistically significantly decreased and DMP1 was slightly decreased (Fig. 2B). Together these data indicated the defective function of osteocytes in *Orai1* −/− mice.

3.3. Defective osteoblastic differentiation and increased proliferation of Orai1 −/− osteoblasts and Orai1 −/− bone marrow cells

To further investigate the role of Orai1 in osteoblast lineage cells at various differentiation stages, *Orai1* −/− primary calvarial osteoblasts (pOBs), which have never been examined in previous studies, and *Orai1* −/− bone marrow stromal cells (BMSCs) were cultured and

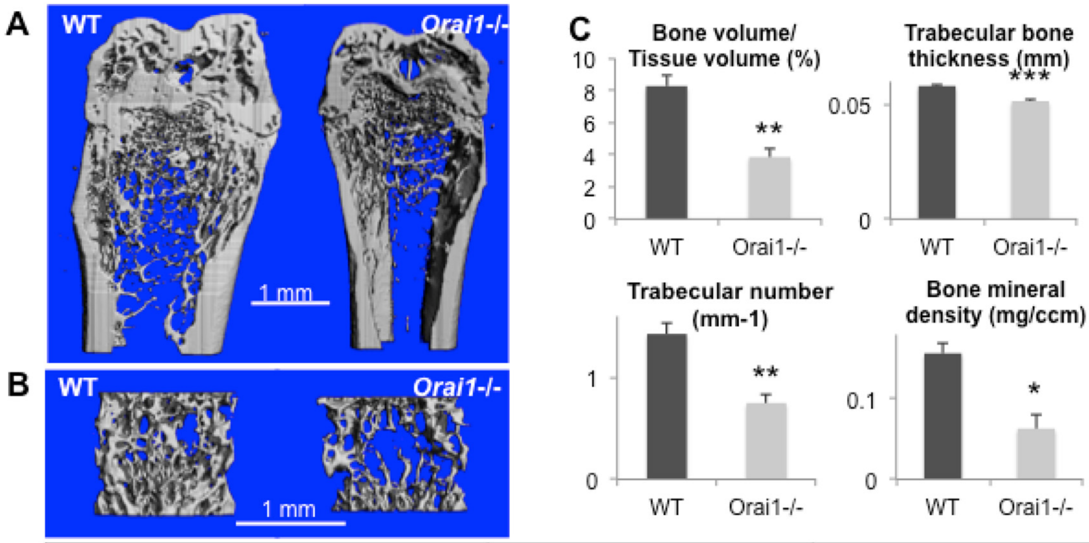

D

	8 week old		12 week old	
	WT	*Orai1-/-*	WT	*Orai1-/-*
Bone volume/total volume (%)	14.86±1.76	9.65±1.13*	8.85±0.51	1.04±0.05**
Osteiod volume/total volume (%)	0.14±0.04	0.23±0.10	0.05±0.03	0.02±0.02
Osteiod volume/bone volume (%)	0.94±0.23	2.23±0.85	0.55±0.31	1.90±1.90
Osteoblast surface/bone surface (%)	11.56±2.44	18.20±3.45*	5.14±4.17	5.85±4.66
Osteoclast surface/bone surface (%)	4.69±1.02	4.93±1.60	0.74±0.54	1.93±1.93
Eroded surface/bone surface (%)	12.00±1.85	10.29±2.39	12.00±1.85	10.29±2.39
Trabecular bone thickness (%)	38.03±2.52	29.44±1.61*	33.81±0.88	18.49±3.94*
Osteoid thickness (%)	2.02±0.38	4.10±1.83	0.97±0.43	0.80±0.80
Osteoblast number/bone perimeter(1/mm)	7.38±1.52	13.69±2.65*	3.08±2.41	6.00±4.91
Osteoclast number/bone perimeter(1/mm)	1.43±0.33	1.65±0.53	0.27±0.21	0.68±0.68
Trabecular separation	228.2±23.78	289.69±28.44*	351.7±30.98	1753.5±292.14*
Trabecular number	3.91±0.34	3.24±0.25	2.63±0.20	0.56±0.12*

Fig. 1. Orai1 deficiency led to age-related bone loss in adult mice.
(A, B) Microcomputed tomography of femurs and lumbar vertebrae. Reconstructed coronal section images of the distal femurs (A) and the lumbar vertebrae (L, B) from WT and Orai1 −/− littermate (8-week old) are shown. (C) Microcomputed tomography three-dimensional structural parameters of the distal metaphyseal area in femurs. ($n = 7$, mean ± SEM, $*p < 0.05$, $**p < 0.01$, $***p < 0.001$;). (D) Bone histomorphometry static parameters of the distal metaphyseal area in femurs from 8 and 12-week old WT and Orai1 −/− mice. ($n = 6$, mean ± SEM, $*p < 0.05$, $**p < 0.01$).

examined for their osteogenic potentials by *in vitro* differentiation assays. *Orai1* −/− pOBs presented significantly reduced Alkaline phosphatase (ALP) positivity, less calcium deposition and fewer nodule formation compared to WT controls, shown by ALP, alizarin red, and von Kossa stainings (Fig. 3A). Correspondingly, osteoblastic marker gene expression - ALP and Osteocalcin (OCN) - were significantly decreased and Orai1 gene expression was ablated in both *Orai1* −/− BMSCs and *Orai1* −/− pOBs, indicated by qPCR analysis (Fig. 3B). Notably, for type I collagen, neither the mRNA expression level (Fig. 3C) nor the intracellular pro-α chain type I collagen protein level was significantly altered in *Orai1* −/− pOBs (Fig. 3D, middle panel), indicating that Orai1 deficiency did not affect the intracellular production of type I collagen protein. However, a significant decrease in extracellular type I collagen protein level in *Orai1* −/− pOBs indicated that Orai1 deficiency affected extracellular secretion of type I collagen in osteoblasts (Fig. 3D, top pannel). As the type I collagen comprises 80% of the unmineralized organic matrix that undergoes mineralization to form bone (Landis and Jacquet, 2013), a significant decrease in extracellular type I collagen can lead to defective bone mineralization. Therefore, defective secretion of type I collagen by *Orai1* −/− osteoblasts may, at least partly, account for significantly decreased bone mineral density and bone mass in *Orai1* −/− mice. Also similarly to *Orai1* −/− pOBs, *Orai1* −/− BMSCs presented decreased expression of osteogenic marker gene ALP and OCN throughout osteogenic differentiation (Fig. 3E). In addition to pOBs, the effect of Orai1 deficiency on BMSCs and mesenchymal progenitors was also examined. The proportional change in the number of mesenchymal progenitors in bone marrow cells of Orai1 −/− mice was examined by colony-forming unit fibroblast (CFU-F). Interestingly, Orai1 −/− cells yielded a significantly higher number of CFU-F, suggesting the increased progenitor population within Orai1 −/− bone marrow cells (Fig 3F and G). Altogether our data suggested a crucial role of Orai1 throughout osteoblast differentiation from mesenchymal progenitors to mineralizing osteoblasts and osteocytes. Meanwhile, the effect of Orai1 deficiency on osteoblast proliferation was also examined by MTT assay and cell counting assay. Assays were performed between one to three days after plating, to access proliferative potential during linear growth prior to confluency. Notably, both MTT assay and cell counting assays indicated significantly upregulated *in vitro* proliferation of *Orai1* −/− pOBs compared to WT (Fig 4A and B). The absorbance value of MTT assay correlated well with the number of both WT and *Orai1* −/− pOBs, therefore MTT assay was valid to examine pOB proliferation (Sup Fig. 2). Taken altogether, these data suggested that Orai1 deficiency affected both differentiation and proliferation of osteoblast lineage cells.

3.4. Defective Ca^{2+}-induced NFAT activation in Orai1 −/− osteoblasts

Finally, to understand the underlying molecular mechanism of defective differentiation and proliferation of *Orai1* −/− osteoblast

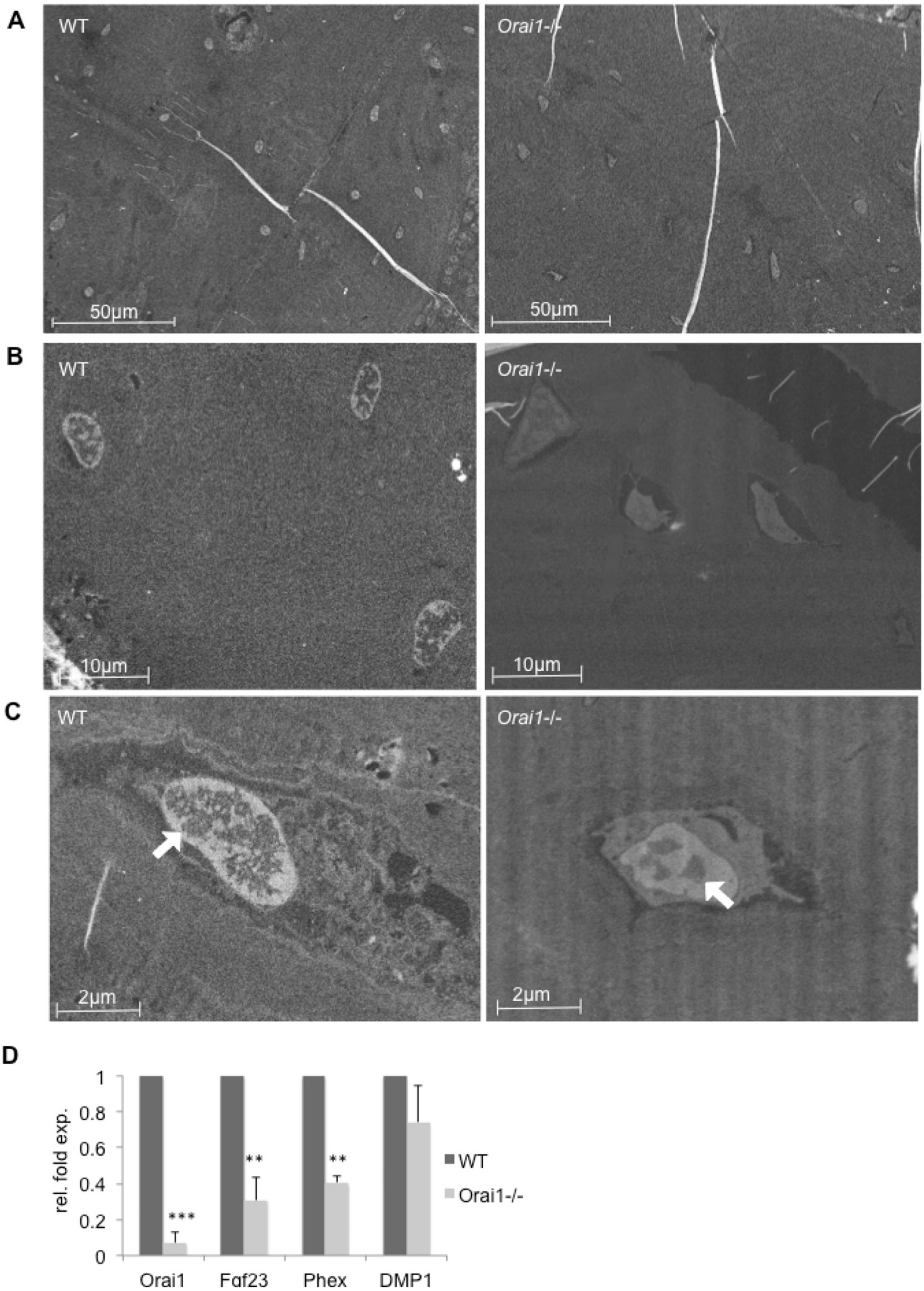

Fig. 2. Orai1 deficiency affected osteocyte morphology and osteocytic gene expression in adult mice.

(A–C) Scanning electron micrograph (SEM) of the femoral compact bone from 8-week old male Orai1 −/− mice (right panels) and male WT littermate control (left panels). In low magnification images (×800(A), ×4,000(B)), Orai1 −/− osteocytes were narrowed and ragged in shape and detached from their lacunae, while WT cells were oval and exhibited no space between the cell and mineralized bone surface. In high magnification SEM (×10,000) images (C), nuclei of Orai1 −/− osteocytes were smaller in size compared to WT. Euchromatin (indicated by white arrows), the electron-lucent areas in nuclei, was significantly less in Orai1 −/− osteocytes, compared to WT.

(D) Osteocytic gene expression in cortical long bone. Changes in mRNA expression of osteoid osteocyte marker gene Phex, mineralizing osteocyte marker gene DMP1 and mature osteocyte marker gene Fgf23 in cortical long bone of 12 week-old Orai1 −/− and WT mice were examined by qRT-PCR. Expression levels normalized to GAPDH are shown as relative fold expression to the WT ($n = 4$, mean ± SEM, $*p < 0.05$, $**p < 0.01$, $***p < 0.001$).

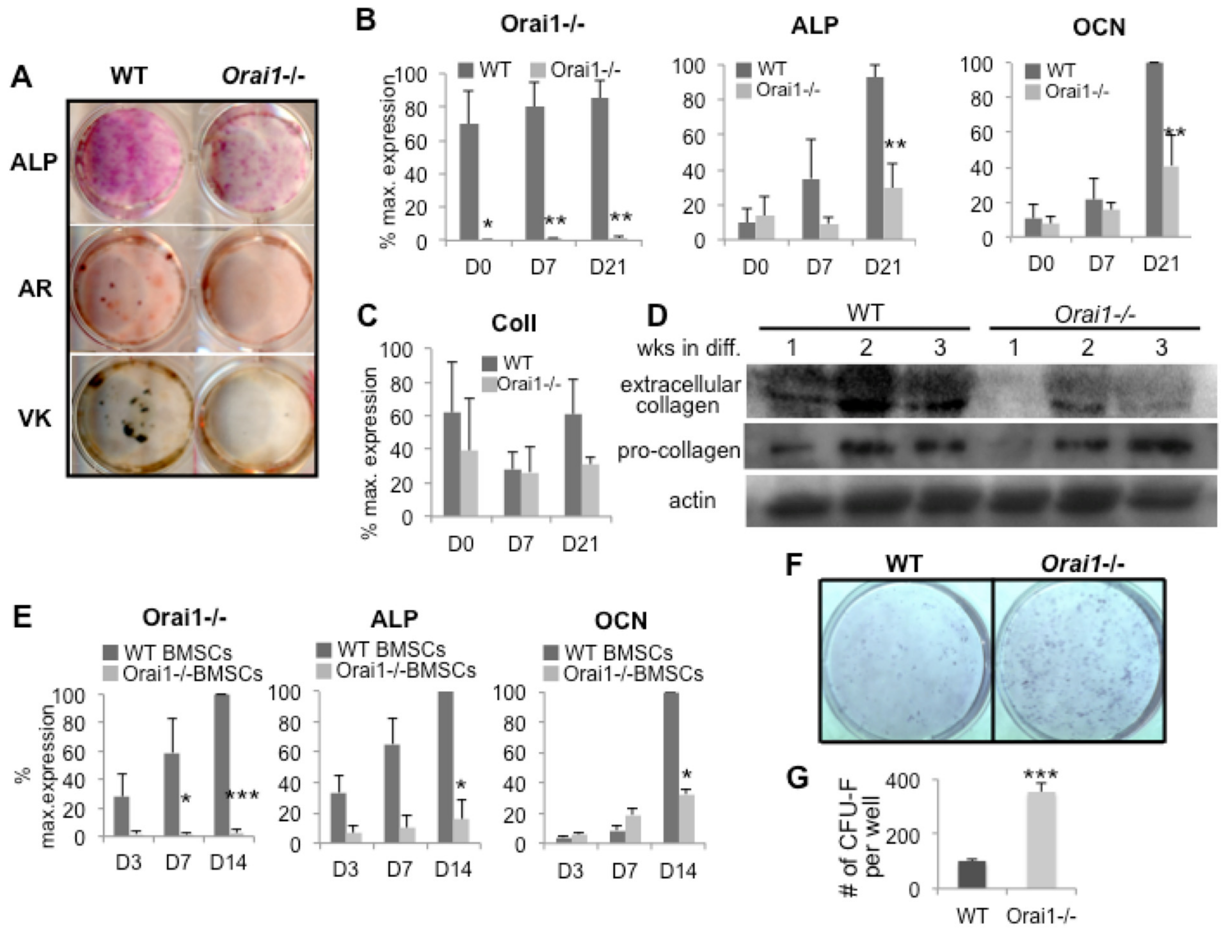

Fig. 3. Orai1 deficiency led to defective function and differentiation of primary calvarial osteoblasts (pOBs) and bone marrow stromal cells (BMSCs).
(A) Representative images of Alkaline Phosphatase (ALP), alizarin red (AR) and Von Kossa (VK) stainings. WT and *Orai1* −/− pOBs were cultured in osteogenic medium for 2 week for ALP and 3 week for AR and VK staining.
(B, C) Osteoblast marker gene expression in pOBs during osteogenic differentiation. Changes in mRNA expression of Orai1, ALP, osteocalcin (OCN) (B) and type I collagen (ColI) (C) in Orai1 −/− and WT pOBs cultured in osteogenic medium for indicated days were examined by qRT-PCR. Values were normalized to GAPDH and shown as the percentage relative to the maximum induction ($n = 3$, mean ± SEM, $^{*}p < 0.05$, $^{**}p < 0.01$, $^{***}p < 0.001$). (D) Western blot analysis of intra and extracellular type I collagen. Orai1 −/− and WT pOBs were cultured in osteogenic condition for indicated days. The protein levels of extracellular mature collagen α chains (ColI) and intracellular collagen pro-α chains (pro-ColI) were examined by Western blot with anti-type I collagen antibody using pepsin-digested extracts and total cell lysates, respectively. Actin served as a loading control for total cell lysates. Representative images from two independent experiments with similar results are shown.
(E) qRT-PCR analysis of osteoblast marker gene expression in Orai1 −/− BMSCs during osteogenic differentiation. Changes in mRNA expression of Orai1, Alkaline Phosphatase (ALP), and osteocalcin (OCN) in Orai1 −/− and WT BMSCs cultured under osteogenic condition were examined by qRT-PCR. Values were normalized to GAPDH and shown as the percentage relative to the maximum induction (n = 3, mean ± SEM, $^{*}p < 0.05$, $^{**}p < 0.01$, $^{***}p < 0.001$) (F) Colony Forming-Unit fibroblast (CFU-F) assay for mesehchymal progenitors. Cells isolated from bone marrow cells were plated for CFU-F assay at very low density (10,000 cells per well of 6 well plate), cultured for 10 days in DMEM supplemented with 20% PBS and 1% P/S, and subjected to Giemsa staining to visualize the colony. Representative images from four independent experiments with similar results are shown. (G) Quantification of CFU-F assay. Colony containing > 50 of Giemsa-positive cells was considered to be CFU-F, and the number of CFU-F per well was counted. ($n = 8$, mean ± SEM, $^{***}p < 0.001$).

lineage cells, we aimed to investigate whether Orai1 deficiency affects SOCE and Ca^{2+}- signaling activation in osteoblasts, as defective SOCE and Ca^{2+}- induced NFAT activation were largely responsible for defective cellular phenotypes of other Orai1 −/− cell types (Gwack et al., 2008; Zhan et al., 2015; Somasundaram et al., 2014; Bikle and Mauro, 2014). Ca^{2+} imaging analysis showed a significant reduction of SOCE in *Orai1* −/− pOBs, indicating a crucial regulatory role of Orai1 for SOCE in osteoblasts (Fig. 5A and Sup Fig. 3). A relatively mild reduction of SOCE in *Orai1* +/− pOBs was shown, indicating a cumulative regulation of SOCE by Orai1 in osteoblasts (Fig. 5A). Also, an immediate attenuation of Ca^{2+} level in WT pOBs by the treatment of 2-aminoethoxydiphenyl borate (2-APB), a SOC channel blocker/Orai1 inhibitor, recapitulated a crucial role of Orai1 in the regulation of intracellular Ca^{2+} level in osteoblasts.

Then, to examine whether NFAT activation is defective in *Orai1* −/− osteoblasts, immunocytochemistry using an antibody against NFATc1 was performed to visualize nuclear accumulation of NFAT, as activated NFAT translocates into the nucleus, where it interacts with other transcription factors and induces downstream gene expression (Winslow et al., 2006; Kawano et al., 2006; Koga et al., 2005). PMA and Ionomycin time-course immunocytochemistry indicated the highest level of nuclear NFAT in WT pOBs at 15 min of treatment (Sup Fig. 4). While > 80% of WT pOBs showed nuclear NFAT after treated with Phorbol myristate acetate (PMA) and Ionomycin for 15 min (Fig. 5B, top panels), only < 20% of *Orai1* −/− pOBs showed nuclear NFAT (Fig. 5B, bottom panels). Furthermore, the effect of Orai1 deficiency on NFAT transcriptional activity was examined by luciferase reporter assay. *Orai1* −/− and WT pOBs were transiently transfected with a luciferase reporter construct containing three tandem repeats of the NFAT-responsive activating protein-1 (AP-1) site in its promoter. PMA

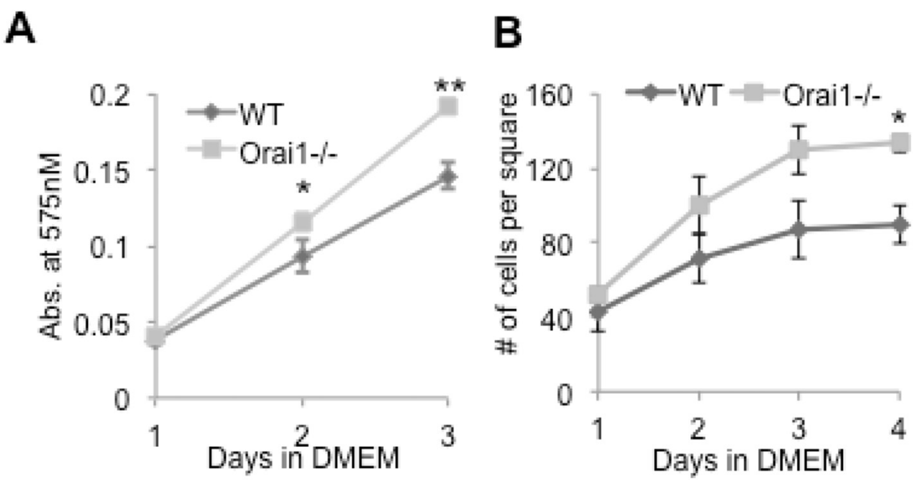

Fig. 4. Orai1 deficiency led to an increase in proliferative potential of primary calvarial osteoblasts (pOBs).

(A) MTT assay of *Orai1* −/− and WT pOBs cultured for indicated days. Cells were plated in triplicates at 20,000 cells per well in 96-well plate. Representative result from three independent experiments with similar results is shown (n = 3, mean ± SEM, *$p < 0.05$, **$p < 0.01$).

(B) Cell counting assay of *Orai1* −/− and WT pOBs cultured for indicated days. Cells were plated at 10,000 cells per well in 12 well plate, cultured, trypsinized, trypan blue-stained for manual counting. Average results from three independent experiments are shown (n = 3, mean ± SEM, *$p < 0.05$).

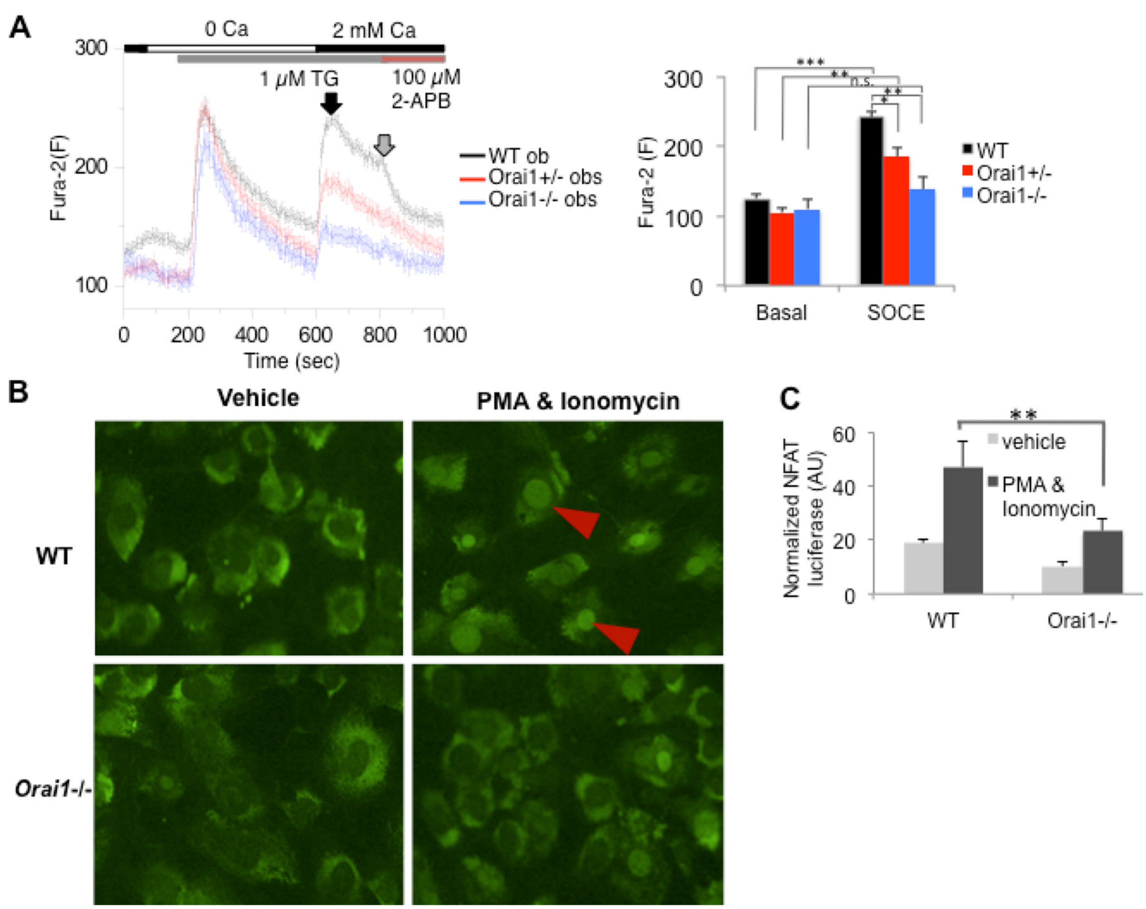

Fig. 5. Orai1 deficiency resulted in defective NFATc1 activation in primary calvarial osteoblasts (pOBs).

(A) Optical imaging of intracellular free Ca^{2+} concentration ($[Ca^{2+}]i$) in WT, Orai1 +/− and Orai1 −/− pOBs. Left panel: The average intensity of Fura-2 fluorescence from 40 cells at different time points is graphically presented with the s.e.m. Cells were loaded with Fura-2 to visualize Ca^{2+}, treated with thapsigargin (TG, 1 μM) in Ca^{2+}-free HEPES-buffered saline solution to induce Store-operated Ca^{2+} entry (SOCE) (black arrow), and with SOC inhibitor 2-APB (100 μM) to block SOCE (gray arrow). Right panel: The bar graph shows the average florescence intensity from 40 cells with s.e.m. at 0 and 650 s. Statistically significant differences were noted between WT, Orai1 +/− and Orai1 −/− pOBs at 650 s.

(B) NFATc1 immunocytochemistry. Cells were treated with PMA (25 nM) and Ionomycin (1 μM) for 15 min to activate Ca^{2+} signaling, fixed, permeabilized, and stained with anti-NFAT antibody followed by FITC-conjugated secondary antibody (green). A decrease in NFATc1 nuclear localization (red arrowhead) was observed in Orai1 −/− pOBs. Representative images from two independent experiments with similar results are shown.

(C) NFATc1 luciferase assay. NFAT transcription activity was evaluated by NFATc1 luciferase assay. WT and Orai1 −/− pOBs were transiently transfected with a luciferase reporter construct containing NFAT-responsive elements in its promoter and treated with PMA (25 nM) and Ionomycin (1 μM) for 6 h. (n = 3, mean ± SEM, **$p < 0.01$). (For interpretation of the references to colour in this figure legend, the reader is referred to the web version of this article.)

and Ionomycin time-course luciferase assay indicated that the luciferase signal peaked at 6 h of treatment (Sup Fig. 5). Importantly, *Orai1* −/− pOBs showed a significant decrease in the luciferase signal both at 0 and 6 h of PMA and Ionomycin treatment, indicating that Orai1 deficiency compromised NFAT transcriptional activity in osteoblasts (*p*-values 0.01 and 0.043, respectively) (Fig. 5C). Together these data suggested that Orai1 deficiency was associated defective Ca^{2+} entry and defective downstream activation of Ca^{2+}- signaling pathways, such as NFAT signaling in osteoblasts.

4. Discussion

Our study highlights the role of Orai1 in bone formation, which occurs *via* the cumulative actions of various osteoblast lineage cells. Our μCT analysis revealed a severe bone loss when Orai1 −/− mice were compared with sex-matched WT littermate controls. As the previous study of adult Orai1 −/− mice reported only a slight bone loss indicating an osteopenic bone phenotype (Hwang et al., 2012), the sex-related differences in bone mass and the genetic variance of Orai1 −/ − mice from outbreeding may account for this disparity between our results and theirs. In particular, our cellular analysis indicated the broad involvement of Orai1 in the function, proliferation, and differentiation of osteoblast lineage cells, reflecting the versatile role of SOCE including the activation of calcium signaling pathways.

The impact of Orai1 deficiency upon osteoblast differentiation has been previously demonstrated by *in vitro* osteogenic differentiation assays using human osteoblast cell line and Orai1 −/− bone marrow stromal cells (Robinson et al., 2012; Hwang et al., 2012; Lee et al., 2016). Herein, we examined various osteoblast lineage cells in Orai1 −/ − mice, such as primary calvarial osteoblasts and osteocytes that have never been examined previously, and demonstrated that Orai1 deficiency broadly impacted the osteoblast lineage differentiation from mesenchymal progenitors to osteocytes. For osteocytes, our data indicated that the involvement of Orai1 in osteocyte biosynthesis, including Fgf23 and Phex gene expression. This corresponds well with a recent study of Zhang et al., which demonstrated the regulation of Fgf23 expression by SOCE and Orai1 in osteoblastic and periosteal cell lines (Zhang et al., 2016).

For osteoblasts, Orai1 affected the main function of osteoblasts, bone matrix deposition such as type I collagen-rich organic matrix. Interestingly, the intracellular protein level of type I collagen in Orai1 −/− osteoblasts was not affected, which indicates that the decrease in extracellular mature type I collagen may be due to defects in intracellular collagen trafficking from ER to plasma membrane or its secretion at the plasma membrane. Concurrent with our observation, Orai1 was recently shown to regulate the exocytosis/secretion of two types of microvesicles - secretory granules and cytotoxic granules in lymphocyte and natural killer cells (Lioudyno et al., 2008; Dickson et al., 2012; Barr et al., 2008; Maul-Pavicic et al., 2011). Although in different cell types, these reports together clearly indicate the involvement of Orai1 in cellular exocytosis/secretion.

While Orai1 has been shown to regulate the differentiation and function of numerous cell types, the role of Orai1 in cellular proliferation has not reached the consensus yet. Gwack et al. showed that Orai1 deficiency led to an increase in CD4+ T cell proliferation (Kim et al., 2011).

However, in keratinocytes, neural progenitor cells, cancer cell lines and proliferating mesenchymal stromal cells, gene deletion or pharmacological/viral inhibition of Orai1 was associated with a decrease in cellular proliferation (Zhan et al., 2015; Somasundaram et al., 2014; Bikle and Mauro, 2014; Maliske et al., n.d.), suggesting that cell-type context is important for the role of Orai1 in cellular proliferation. *In vitro* test results for osteoblast proliferation were inconsistent as well among groups. A previous study by Hwang et al., showed an insignificant impact of Orai1 upon proliferation of MC3T3 osteoblast cell line (Hwang et al., 2012). In that study, the authors used dominant-negative Orai1 expressing cells in comparison to WT controls and performed MTT assay one to two weeks after cell plating. Our MTT assay, however, clearly indicated an increase in *in vitro* proliferation of primary Orai1 −/− osteoblasts when their proliferative potential was accessed during the linear growth phase of cells, which was between one to three days after plating before cells reach the confluency. For *in vivo* proliferation, a study by Robinson et al. showed a decrease in the positive ALP labeled area on the vertebrae of Orai1 −/− mice (Robinson et al., 2012). Interestingly, our histomorphometry indicated an increase in osteoblast number per bone perimeter and an increase in osteoblast area per bone area in Orai1 −/− mice. As ALP-positivity is a marker of active/mature osteoblasts, the results of ours and Robinson et al. together may indicate the increased proliferation of ALP-negative premature osteoblasts and/or overall delayed differentiation of osteoblasts in Orai1 −/− mice.

The diverse effects of Orai1 deficiency on osteoblast secretion, proliferation, and differentiation are not surprising, given the versatile role of intracellular calcium in osteoblast biology. Orai1 can possibly mediate the activation of signaling pathways utilizing Ca^{2+}, such as protein kinase C, BMP, Wnt, TGF- β1, calmodulin, and calcineurin/NFAT signaling pathways, all of which take crucial roles in various osteoblast functions, including differentiation and proliferation (Winslow et al., 2006; Kawano et al., 2006; Koga et al., 2005; Lee et al., 2016; Choo et al., 2009; Blair et al., 2007; Kohn and Moon, 2005). Moreover, defective Ca^{2+-}entry resulted from defective Orai1 may disrupt intracellular calcium kinetics in ER and other calcium-mediating compartments, such as mitochondria and lysosomes, which mediate a variety of osteoblastic cellular functions such as metabolism, survival, apoptosis, secretion and differentiation (Zhao et al., 2008; Koizumi et al., 2003; Mahamid et al., n.d.; Sato et al., 2015; Cabral et al., 2016).

Altogether, our study addressed the importance of the calcium channel Orai1 and intracellular calcium homeostasis in osteoblast lineage cells, from mesenchymal progenitors to osteocytes. Further studies on how Orai1 affects the activation of various calcium signaling pathways and the calcium-mediating intracellular compartments in osteoblasts lineage cells, will allow us to better understand the molecular regulation mechanism of osteoblast functions of proliferation and differentiation as well as bone homeostasis.

Transparency document

The Transparency document associated with this article can be found, in online version.

Acknowledgements

This research was supported by the National Institutes of Health grants AI-083432, AI-088393 (to Y.G) and R01 DE019465 (to S.T).

Appendix A. Supplementary data

Supplementary data to this article can be found online at https://doi.org/10.1016/j.bonr.2018.03.007.

References

Aghaloo, T.L., et al., Periodontal disease and bisphosphonates induce osteonecrosis of the jaws in the rat. J. Bone Miner. Res. 26(8): p. 1871–1882.
Aghaloo, T.L., et al., Osteogenic potential of mandibular vs. long-bone marrow stromal cells. J. Dent. Res. 89(11): p. 1293–1298.
Alcobendas, M., Baud, C., Castanet, J., 1991. Structural changes of the periosteocytic area in *Vipera aspis* (L.) (Ophidia, Viperidae) bone tissue in various physiological conditions. Calcif. Tissue Int. 49 (1), 53–58.
Barr, V.A., et al., 2008. Dynamic movement of the calcium sensor STIM1 and the calcium channel Orai1 in activated T-cells: puncta and distal caps. Mol. Biol. Cell 19 (7), 2802–2817.
Bikle, D.D., Mauro, T., 2014. Calcium, Orai1 and epidermal proliferation. J. Invest.

Dermatol. 134 (6), 1506–1508.
Blair, H.C., et al., 2007. Calcium signalling and calcium transport in bone disease. Subcell. Biochem. 45, 539–562.
Cabral, W.A., et al., 2016. Absence of the ER cation channel TMEM38B/TRIC-B disrupts intracellular calcium homeostasis and dysregulates collagen synthesis in recessive osteogenesis imperfecta. PLoS Genet. 12 (7), e1006156.
Choo, M.-K., Yeo, H., Zayzafoon, M., 2009. NFATc1 mediates HDAC-dependent transcriptional repression of osteocalcin expression during osteoblast differentiation. Bone 45 (3), 579–589.
Dallas, S.L., Prideaux, M., Bonewald, L.F., 2013. The osteocyte: an endocrine cell and more. Endocr. Rev. 34 (5), 658–690.
Dickson, E.J., et al., 2012. Orai-STIM–mediated Ca^{2+} release from secretory granules revealed by a targeted Ca^{2+} and pH probe. Proc. Natl. Acad. Sci. 109 (51), E3539–E3548.
Feske, S., Gwack, Y., Prakriya, M., Srikanth, S., Puppel, S.H., Tanasa, B., Hogan, P.G., Lewis, R.S., Daly, M., Rao, A., 2006. A mutation in Orai1 causes immune deficiency by abrogating CRAC channel function. Nature 441 (7090), 179–185.
Gwack, Y., et al., 2008. Hair loss and defective T- and B-cell function in mice lacking ORAI1. Mol. Cell. Biol. 28 (17), 5209–5222.
Hsu, W.K., et al., 2008. Characterization of osteolytic, osteoblastic, and mixed lesions in a prostate cancer mouse model using 18F-FDG and 18F-fluoride PET/CT. J. Nucl. Med. 49 (3), 414–421.
Hwang, S.-Y., Putney, J.W., 2012. Orai1-mediated calcium entry plays a critical role in osteoclast differentiation and function by regulating activation of the transcription factor NFATc1. FASEB J. 26 (4), 1484–1492.
Hwang, S.-Y., et al., 2012. Deletion of Orai1 alters expression of multiple genes during osteoclast and osteoblast maturation. Cell Calcium 52 (6), 488–500.
Kawano, S., et al., 2006. ATP autocrine/paracrine signaling induces calcium oscillations and NFAT activation in human mesenchymal stem cells. Cell Calcium 39 (4), 313–324.
Kim, K.-D., et al., 2011. ORAI1 deficiency impairs activated T cell death and enhances T cell survival. J. Immunol. 187 (7), 3620–3630.
Koga, T., et al., 2005. NFAT and Osterix cooperatively regulate bone formation. Nat. Med. 11, 880–885.
Kohn, A.D., Moon, R.T., 2005. Wnt and calcium signaling: β-catenin-independent pathways. Cell Calcium 38 (3–4), 439–446.
Koizumi, T., et al., 2003. Cell density and growth-dependent down-regulation of both intracellular calcium responses to agonist stimuli and expression of smooth-surfaced endoplasmic reticulum in MC3T3-E1 osteoblast-like cells. J. Biol. Chem. 278 (8), 6433–6439.
Kronenberg, H.M., 2016. Bone and mineral metabolism: where are we, where are we going, and how will we get there? J. Clin. Endocrinol. Metab. 101 (3), 795–798.
Landis, W.J., Jacquet, R., 2013. Association of calcium and phosphate ions with collagen in the mineralization of vertebrate tissues. Calcif. Tissue Int. 93 (4), 329–337.
Lee, S.H., et al., 2016. Orai1 mediates osteogenic differentiation via BMP signaling pathway in bone marrow mesenchymal stem cells. Biochem. Biophys. Res. Commun. 473 (4), 1309–1314.
Lioudyno, M.I., et al., 2008. Orai1 and STIM1 move to the immunological synapse and are up-regulated during T cell activation. Proc. Natl. Acad. Sci. 105 (6), 2011–2016.
Mahamid, J., et al., Bone mineralization proceeds through intracellular calcium phosphate loaded vesicles: a cryo-electron microscopy study. J. Struct. Biol. 174(3): p. 527–535.
Maliske, J.K., et al., 2012. Store-operated calcium entry regulate mesenchymal stem cell proliferation. FASEB J. 26 (1 Supplement), 571–574.
Maul-Pavicic, A., et al., 2011. ORAI1-mediated calcium influx is required for human cytotoxic lymphocyte degranulation and target cell lysis. Proc. Natl. Acad. Sci. 108 (8), 3324–3329.
Ono, N., Kronenberg, H.M., 2015. Mesenchymal progenitor cells for the osteogenic lineage. Curr. Mol. Biol. Rep. 1 (3), 95–100.
Palumbo, C., 1986. A three-dimensional ultrastructural study of osteoid-osteocytes in the tibia of chick embryos. Cell Tissue Res. 246 (1), 125–131.
Pirih, F.Q., et al., 2008. Nuclear receptor profile in calvarial bone cells undergoing osteogenic versus adipogenic differentiation. J. Cell. Biochem. 105 (5), 1316–1326.
Robinson, L.J., et al., 2012. Gene disruption of the calcium channel Orai1 results in inhibition of osteoclast and osteoblast differentiation and impairs skeletal development. Lab. Investig. 92 (7), 1071–1083.
Sato, A.Y., et al., 2015. Prevention of glucocorticoid induced-apoptosis of osteoblasts and osteocytes by protecting against endoplasmic reticulum (ER) stress in vitro and in vivo in female mice. Bone 73, 60–68.
Soleimani, M., Nadri, S., 2009. A protocol for isolation and culture of mesenchymal stem cells from mouse bone marrow. Nat. Protoc. 4 (1), 102–106.
Somasundaram, A., et al., 2014. Store-operated CRAC channels regulate gene expression and proliferation in neural progenitor cells. J. Neurosci. 34 (27), 9107–9123.
Tetradis, S., Bezouglaia, O., Tsingotjidou, A., 2001. Parathyroid hormone induces expression of the nuclear orphan receptor Nurr1 in bone cells. Endocrinology 142 (2), 663–670.
Winslow, M.M., et al., 2006. Calcineurin/NFAT signaling in osteoblasts regulates bone mass. Dev. Cell 10 (6), 771–782.
Wysolmerski, J.J., 2013. Osteocytes remove and replace perilacunar mineral during reproductive cycles. Bone 54 (2), 230–236.
Zhan, Z.-Y., et al., 2015. Over-expression of Orai1 mediates cell proliferation and associates with poor prognosis in human non-small cell lung carcinoma. Int. J. Clin. Exp. Pathol. 8 (5), 5080–5088.
Zhang, B., et al., 2016. NFκB-sensitive Orai1 expression in the regulation of FGF23 release. J. Mol. Med. 94 (5), 557–566.
Zhao, H., et al., 2008. Synaptotagmin VII regulates bone remodeling by modulating osteoclast and osteoblast secretion. Dev. Cell 14 (6), 914–925.